Isoprenylated Flavonoids and 2-Arylbenzofurans from the Root Bark of Morus alba L. and Their Cytotoxic Activity of against HGC27 Cancer Cells

Hang Yi Pu , Dong Yi Cao , Xue Zhou , Fu Li , Lun Wang , Ming Kui Wang *

Posted Date: 21 November 2023

doi: 10.20944/preprints202311.1185.v1

Keywords: Morus alba L.; gastric cancer; HGC27 cells; cytotoxic activities

Article

Isoprenylated Flavonoids and 2-Arylbenzofurans from the Root Bark of *Morus alba* L. and Their Cytotoxic Activity of against HGC27 Cancer Cells

Hang-Yi Pu [a,b], Dong-Yi Cao [c], Xue Zhou [a,b], Fu Li [a,b], Lun Wang [a,b] and Ming-Kui Wang [a,b,*]

[a] Natural Products Research Center, Chengdu Institute of Biology, Chinese Academy of Sciences, Chengdu 610041, China
[b] University of Chinese Academy of Sciences, Beijing 100049, China
[c] The Third Affiliated Hospital of Yunnan University of Chinese Medicine, Kunming 650500, Yunnan, China
* Correspondence: wangmk@cib.ac.cn; Tel./Fax: +86-28-82890821

Abstract: Three new compounds (**1**, **11** and **12**), together with 32 known ones, were isolated from the root bark of *Morus alba* L. using various chromatographic methods. The structures of the undescribed compounds were elucidated based on 1D, 2D NMR and HRESIMS data analysis, while the known ones were identified by comparison of their spectroscopic data with those reported in the literature. All the isolates were evaluated for their cytotoxic activities against human gastric cancer HGC27 cells by CCK-8 assay. Among them, compounds **5**, **8**, **10** and **30** exhibited cytotoxic activities on HGC27 cells with IC_{50} values of 10.24 ± 0.89 μM, 28.94 ± 0.72 μM, 6.08 ± 0.34 μM and 33.76 ± 2.64 μM, respectively. Furthermore, compound **10** was confirmed to reduce proliferation ability, increase apoptosis rate and inhibit cell migration pathway by annexin V/PI double staining experiment, transwell experiment and western blot analysis.

Keywords: *Morus alba* L.; gastric cancer; HGC27 cells; cytotoxic activities

1. Introduction

Morus alba L., the root bark of *Morus* mulberry, is a well-known traditional Chinese medicine (TCM) documented in Chinese Pharmacopoeia [1]. The root bark of *M. alba* has been widely used in Chinese herbal medicinal prescriptions for the treatment of pneumonia, hypertension, diabetes, arthritis [2,3]. Previous phytochemical studies revealed that *M. alba* contained a variety of polyphenolic constituents such as prenylated flavonoids, 2-arylbenzofurans, stilbene, coumarin and mulberry diels-alder-type adducts. In addition, Pharmacological studies exhibited that some polyphenols from *M. alba* had a broad spectrum of biological activities, such as hepatoprotective activity, whitening ability, and antiplatelet effects [4–9]. Previous studies also showed that diverse individual compounds or extracts from different parts of various mulberry plants (*M. alba, M. australis, M. wittiorum and M. yunanensis*) exhibited anti-tumor activity against different tumor cell lines, such as lung cancer, liver cancer, colon cancer, breast cancer, rectal adenocarcinoma, and renal adenocarcinoma [10–14]. Our preliminary pharmacological experiment showed that the 75% ethanol extract of *M. alba* exhibited certain anti-tumor activity against gastric cancer cells, which had rarely been reported. Thus, the present paper focuses on detailed phytochemical investigation of the 75% ethanol extract of *M. alba* and evaluation of anti-tumor activity against gastric cancer cells of the isolated individual compounds. As a result, thirty five compounds including three new ones were obtained. Among them, compound **10** (Albanol B) showing the most significant cytotoxicity with an IC_{50} value of 6.08 ± 0.34 μM. Moreover, the potential mechanism was preliminarily explored.

 doi:10.20944/preprints202311.1185.v1

2. Results and discussion

2.1. Isolation and Structure Elucidation

Phytochemical investigation on the 75% ethanol extract of the root bark of *M. alba* led to the isolation and identification of three new compounds (**1**, **11** and **12**) and 32 known compounds (**2–10**, **13–35**) as shown in Figure 1.The known compounds were identified by comparing their NMR and ESIMS data with those reported in the literature as mulberrofuran D (**2**) [17], Mulberofuran B (**3**) [18], Mulberofuran A (**4**) , Albafuran A (**5**) [20], Mulberrofuran Y (**6**) [21], Moracin M (**7**) [22], Mulberrofuran G (**8**) [23], Mulberrofuran J (**9**) [24], Albanol B (**10**) [25]. Kuwanon T (**13**) [23], Morusin (**14**) [18], KuwanonA (**15**) [26], Notabilisin L (**16**) [27], 14-Methoxydihydromorusin (**17**) [28], Neocyclomorusin (**18**) [29], Cyclomulberrin (**19**) [30], Cyclomorusin (**20**) [29], Artoflavone (**21**) [31], Cudraflavone A (**22**) [32], Kuwanon C (**23**) [33], Mornigrol H (**24**) [34], Austraone A (**25**) [35], Sanggenol Q (**26**) [36], Cycloaltilisin 7 (**27**) [37], Sanggenol O (**28**) [23], Kuwanon E (**29**) [29], Benzokuwanon E (**30**) [38], Kuwanon G (**31**) [18], Albanin G (**32**) [39], Moracenin D (**33**) [40], Mulberrofuran P (**34**) [41], 7,4'-Dihydroxyflavone (**35**) [42].

Compound **1** was obtained as a brown amorphous powder. The molecular formula of **1** was determined as $C_{25}H_{28}O_5$ according to its HR-ESI-MS at *m/z* 438.1831 $[M + Na]^+$ (calcd. for $C_{25}H_{28}O_5Na$, 438.1829), indicating the presence of 12 degrees of unsaturation. Absorption maxima in the UV spectrum of **1** at λ_{max} 216 (4.21) and 316 (4.19) nm suggested that it was a 2-arylbenzofuran derivative [43]. In the ^{1}H NMR spectrum (Table 1), three methyl groups at δ_H 1.62 (3H, s, H-10″), 1.89 (3H, s, H-4″), 3.86 (3H, s, -OCH_3); four methylenes at δ_H 1.60 (2H, m, H-6″), 2.02 (2H, m, H-5″), 3.62 (2H, d, *J* = 7.2, H-1″), 4.79, 4.72 (2H, s, H-9″α, β); an olefinic singlet at δ_H 6.92 (1H, s, H-3), two aromatic doublet signals at δ_H 7.32 (1H, d, *J* = 8.4, H-4), δ_H 6.90 (1H, d, *J* = 8.4, H-5), a 1, 3, 5-trisubstituted aromatic system (ring B) at δ_H 6.80 (2H, d, *J* = 2.0, H-2′, 6′) and δ 6.26 (1H, s, H-4′) were observed. The ^{13}C NMR (Table 1), DEPT and HSQC spectra showed 25 carbon signals, including three methyls, four methylenes, eight methines, and ten quaternary carbons. Comparison of the ^{1}H and ^{13}C-NMR spectral data of **1** with those of mulberofuran B (**3**) indicated that they shared similar chemical structures [18]. The marked difference occurred in the position of C-7″ of the geranyl group. The carbon signals for C-5″and C-7″ were shifted downfield to δ_C 36.7 (-4.2 ppm) and 76.1 (-49.3 ppm), while the C-6″, C-8″ and C-9″ signals in **1** were shifted upfield dramatically to δ_C 34.2 (+6.5 ppm), 148.6 (+16.3 ppm) and 111.5 (+85.7 ppm) (Table 1), respectively. Signals in the upfield of the ^{1}H NMR spectrum of **1** were deduced to be a changed geranyl group, one of whose double bonds was hydrated. Two proton signals at δ_H 4.72 (1H, s) and 4.79 (1H, s) and a signal at δ_H 3.90 (1H, t, *J* = 6.8 Hz) suggested that a terminal methylene group and an oxygen-bearing methine group were present in the geranyl group. According to the HSQC spectrum that δ_C 111.5 and δ_C 76.1 was connected with δ_H 3.90 (1H, t, *J* = 6.8 Hz), δ_H 4.79 (1H, brs) and 4.72 (1H, s), respectively. In the HMBC spectrum (Figure 2), long-range correlations of H-9″/C-7″, 10″ and H-7″/C-5″, 9″, 10″, demonstrated that the geranyl group was replaced by a 7″-hydroxy-3″, 8″-dimethylbut-2″, 8″dioctenyl group [44]. Furthermore, H-1″ showed long-range correlations with C-6 and C-7a, supporting that the changed geranyl group was located at C-7. According to the above NMR data analysis, compound **1** (shown in Figure 1) was elucidated as 7″-hydroxy-3″, 8″-dimethylbut-2″, 8″-dioctenyl- 6-methoxy- 3′, 5′-dihydroxy-2-arylbenzofuran, and was named mulberofuran Z.

Compound **11** was obtained as a yellow powder. The molecular formula of **11** was determined as $C_{25}H_{26}O_7$ according to its HR-ESI-MS at *m/z* 439.1751 $[M + H]^+$ (calcd. for $C_{25}H_{27}O_7$, 439.1751), indicating 13 degrees of unsaturation. The IR spectrum exhibited absorption peaks attributable to hydroxy groups (3415 cm^{-1}), a conjugated carbonyl group (1656 cm^{-1}), and aromatic rings (1621, 1554, 1448 cm^{-1}). In the ^{1}H NMR spectrum, signals due to an isopentyl group at δ_H 1.61 (3H, s, CH_3-4″), 1.71 (3H, s, CH_3-5″), 3.36 (2H, d, *J* = 6.0 Hz, H-1″), and 5.13 (1H, brt, *J* = 6.0 Hz, H-2″) were observed. The ^{1}H NMR spectrum also showed ortho-coupled aromatic protons (ring B) at δ_H 7.67 (1H,d, *J* = 9.0 Hz, H-6′), 6.74 d (1H, d, *J* = 9.0 Hz, H-5′) and meta-coupled aromatic protons (ring A) at δ_H 6.12 (1H, brs, H-6), 6.33 (1H, brs, H-8). Two methyl groups δ_H 1.18 (3H, s, CH_3-12), 1.29 (3H, s, CH_3-13) and an AMX coupling system at δ_H 2.74 (1H, dd, *J* = 16.2, 6.0 Hz, H-9α), 3.00 (1H, dd, *J* = 16.2, 3.6 Hz, H-9β) and 3.99 (1H, dd, *J* = 6.0, 3.6 Hz, H-10) indicated the existence of an oxepin ring [45]. The ^{13}C NMR, DEPT

Preprints (www.preprints.org) | NOT PEER-REVIEWED | Posted: 21 November 2023 doi:10.20944/preprints202311.1185.v1

and HSQC spectra showed the presence of 25 carbons, including 4 methyl, 2 methylene, 6 methylene and 13 quaternary carbons. Comparison of the ^{1}H NMR and ^{13}C NMR data of compound **11** with those of the known compound artoxanthocarpuone A suggested that the difference between them was the location of the isopentyl group at C-3′ in **11** rather than at C-6 in artoxanthocarpuone A, which was further confirmed by the key long range correlations from δ_H 3.36 (H-1″) to δ_C 159.4 (C-2′), 119.9 (C-3′), 156.4 (C-4′) and 130.3 (C-3″) (Figure 2). Based on these observations, compound **11** can be assigned as shown in Figure 1 and named as artoxanthocarpuone C.

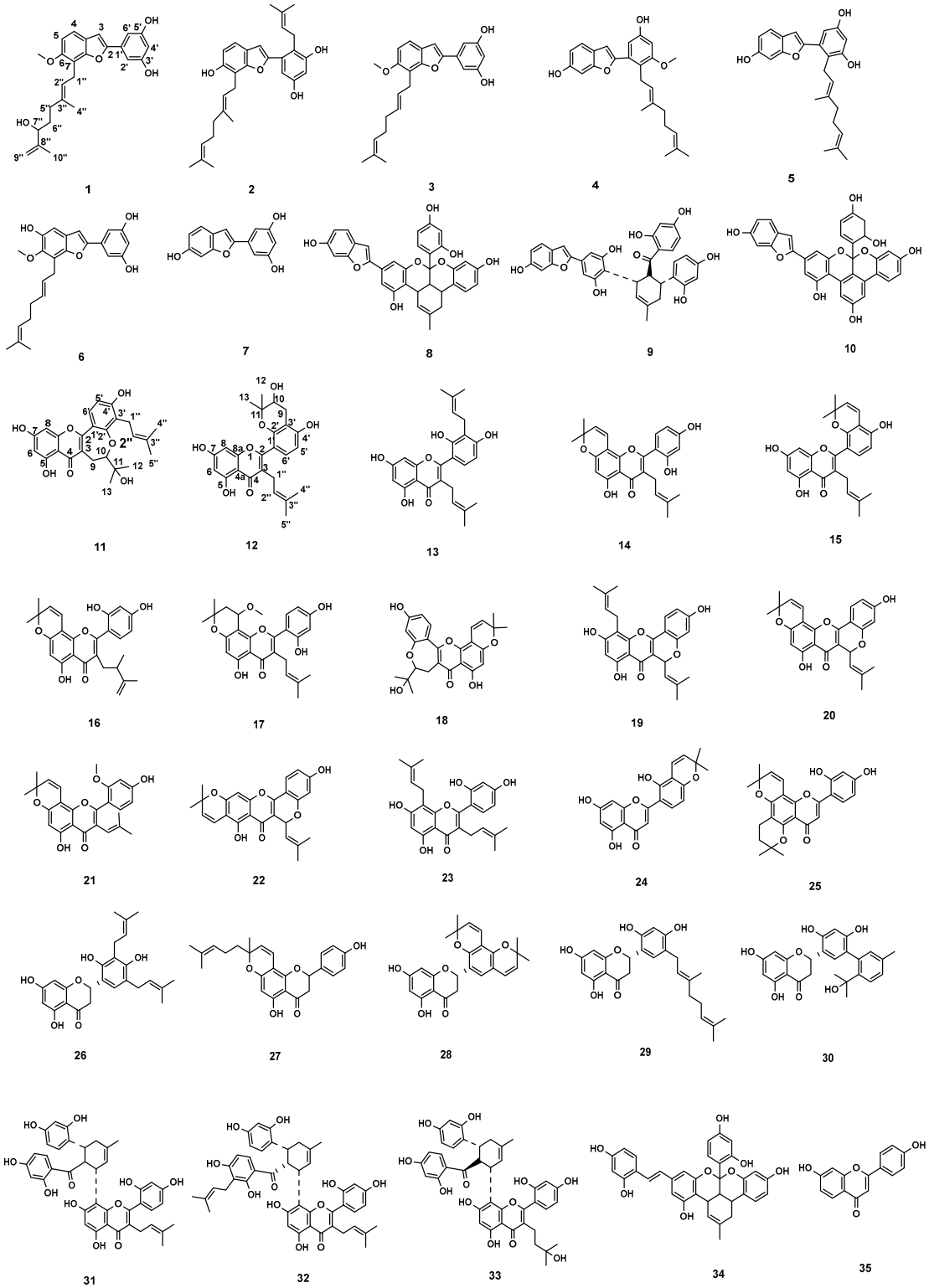

Figure 1. Chemical structures of compounds **1–35.**

Preprints (www.preprints.org) | NOT PEER-REVIEWED | Posted: 21 November 2023 doi:10.20944/preprints202311.1185.v1

Table 1. ^{1}H NMR (400 MHz) and ^{13}C NMR (100 MHz) data of **1** in CD_3OD (δ in ppm, J in Hz). (*) refers to overlapped signals.

No.	δ_H (J in Hz)	δ_C	No.	δ_H (J in Hz)	δ_C
2		156.7	1″	3.62 d (7.2)	23.6
3	6.92 s	102.3	2″	5.40 t (7.2)	123.6
3a		124.2	3″		135.9
4	7.32 d (8.4)	119.1	4″	1.89 s	16.4
5	6.90 d (8.8)	109.3	5″	2.02 m	36.7
6		156.4	6″	1.60 m	34.2
7		114.4	7″	3.90 t (6.8)	76.1
7a		155.3	8″		148.6
1′		133.8	9″α	4.79 s	111.5
2′	6.80* d (2.0)	104.1	9″β	4.72 s	
3′		160.0	10″	1.62 s	17.5
4′	6.26 s	103.6	-OCH3	3.86 s	57.0
5′		160.0			
6′	6.80* d (2.0)	104.1			

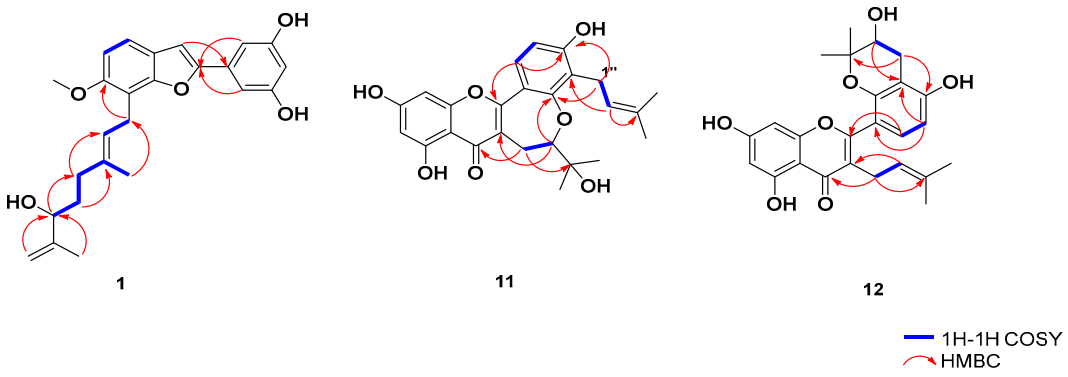

Figure 2. The ^{1}H-^{1}H COSY and key HMBC correlations of compounds **1, 11**and**12.**

Compound **12** was obtained as a yellow powder. The molecular formula of **12** was determined as $C_{25}H_{26}O_7$ according to its HR-ESI-MS at m/z 439.1749 $[M + H]^+$ (calcd. for $C_{25}H_{27}O_7$, 439.1751), indicating 13 degrees of unsaturation. The IR spectrum exhibited absorption peaks attributable to hydroxy groups (3372 cm^{-1}), a conjugated carbonyl group (1645 cm-1). The UV spectrum showed absorbance maxima at 336 and 215 nm, typical of a flavone skeleton. The ^{1}H NMR spectrum clearly exhibited the presence of an isopentyl group at δ_H 1.34 (3H, s, CH_3-4″), 1.58 (3H, s, CH_3-5″), 3.08 (2H, dd, J = 7.2, 5.4 Hz, H-1″), and 5.07 (1H, t, J = 7.2 Hz, H-2″). The ^{1}H NMR spectrum also showed ortho-coupled aromatic protons (ring B) at δ_H 6.98 (1H, d, J = 8.4 Hz, H-6′), 6.42 (1H, d, J = 8.4 Hz, H-5′) and meta-coupled aromatic protons (ring A) at δ_H 5.91 (1H, s, H-6), 6.00 (1H, s, H-8). Two methyl groups δ_H 1.36 (3H, s, CH_3-12), 1.28 (3H, s, CH_3-13) and an AMX coupling system at δ_H 2.61 (1H, dd, J = 16.8,

Preprints (www.preprints.org) | NOT PEER-REVIEWED | Posted: 21 November 2023 doi:10.20944/preprints202311.1185.v1

5.4 Hz, H-9a), 2.95 (1H, dd, *J* = 16.8, 7.4 Hz, H-9b), and 3.80 (1H, dd, *J* = 16.2, 5.4 Hz, H-10) indicated the existence of an oxepin ring [45]. The ^{1}H NMR and ^{13}C NMR spectra of **12** were similar to those of the known compound kuwanon A [26]. The carbon signals at δ_C 70.2 (C-10) and 27.6 (C-9) in **12** instead of δ_C 128.9 (C-10) and 116.3 (C-9) in kuwanon A, along with the difference of their molecular weight, demonstrated the presence of a hydroxy group at C-10 in **12**. This was further verified by the long-range correlations from H-9 to C-11, C-1′ and C-4′ and from H-10 to C-11 and C-3′ in the HMBC spectrum (Figure 2) [46]. The HMBC correlations of H-1″/C-2, C-4 and H-2″/C-3, C-4″, C-5″ suggested the isopentyl group was attached to C-3 position. According to the above data, compound **12** was established as depicted in Figure 1 and named as kuwanon Z.

2.2. Biological activities of compounds against HGC27 cancer cells

The effect of compounds (**1**–**35**) on the cell viability of HCG27 cells was evaluated by CCK-8 assay. As shown in Table 3, four compounds **5**, **8**, **10** and **30** had a better significant inhibitory effect on the viability of HCG27 cells compared with the model group (control). In contrast, other compounds had no significant inhibitory effects on the viability of HCG27 cells, therefore, compounds **5**, **8**, **10** and **30** were screened to evaluate the semi-inhibition concentration (IC_{50}) values (Table 4). Among the four compounds, compound **10** showed the best cytotoxicity against HCG27 cells, with an IC_{50} value of 6.08±0.34 μM, and compounds **5**, **8** and **30** showed weaker cytotoxic activities, with IC_{50} values of 10.24 ± 0.89 μM, 28.94 ± 0.72 μM and 33.76 ± 2.64 μM, respectively. Compound **10** effectively inhibited the clone formation of HGC27 cells (Figure 3a). When cells were treated with 20 μM compound **10**, the number of cell clones formed in the administered group was significantly reduced and cell growth was significantly inhibited compared to the control group (Figure 3b). This suggests that compound **10** may cause apoptosis. We used Annexin V-FITC (Annexin V-Fluorescein Isothiocyanate) double staining assay to detect apoptotic cells. As shown in Figure 3c, the apoptosis rate of HGC27 cells treated with compound **10** significantly increased compared to the control group. Quantification of apoptotic cells by flow cytometry revealed that the percentage of HGC27 apoptotic cells increased in a dose-dependent manner (Figure 3d).

Table 2. ^{1}H NMR and ^{13}C NMR data for the compounds **11** and **12** (δ in ppm, *J* in Hz).

	11[a]		**12**[b]	
No.	δ_H (*J* in Hz)	δ_C	δ_H (*J* in Hz)	δ_C
2		158.6		163.1
3		115.7		122.1
4		179.7		183.1
4a		102.0		105.4
5		157.3		163.2
6	6.12 brs	98.9	5.91[a] s	99.7[a]
7		161.3		165.8
8	6.33 brs	93.6	6.00[a] s	94.0[a]
8a		157.3		157.1
9α	2.74 dd (16.2, 6.0)	23.0	2.61 dd (16.8, 5.4)	27.5
9β	3.00 dd (16.2, 3.6)		2.95 dd (16.8, 7.4)	
10	3.99 dd (6.0, 3.6)	91.5	3.80 dd (16.2, 6.0)	70.2
11		70.9		78.1
12	1.18 s	27.3	1.36 s	25.8
13	1.29 s	24.1	1.28 s	20.8

Preprints (www.preprints.org) | NOT PEER-REVIEWED | Posted: 21 November 2023 doi:10.20944/preprints202311.1185.v1

1′		114.0		113.8
2′		159.4		154.7
3′		119.9		110.3
4′		156.4		157.0
5′	6.74 d (9.0)	110.7	6.42 d (8.4)	109.9
6′	7.67 d (9.0)	126.8	6.98 d (8.4)	129.5
1″	3.36*d (6.0)	22.5	3.08 dd (7.2, 5.4)	24.8
2″	5.13 t (7.2)	123.2	5.07 t (7.2)	122.6
3′		130.3		132.8
4″	1.61 s	25.5	1.34 s	17.6
5″	1.71.s	17.9	1.58 s	25.8
5-OH	13.02 s			

[a] recorded at 600 (150) MHz in DMSO. [b] recorded at 600 (150) MHz in CD_3OD. (*) refers to overlapped signals.

Table 3. Cell viability of Compounds **1**-**35** on HGC27 cells.

Compound	Cell viability (%)	Compound	Cell viability (%)
1	96.42 ± 4.57	**19**	95.67 ± 3.65
2	97.88 ± 2.26	**20**	93.72 ± 2.86
3	96.27 ± 2.37	**21**	98.96 ± 0.92
4	92.08 ± 4.25	**22**	96.86 ± 1.84
5	98.38 ± 0.58	**23**	83.99 ± 3.92
6	89.04 ± 3.06	**24**	94.57 ± 2.74
7	89.47 ± 2.04	**25**	88.99 ± 4.62
8	59.92 ± 2.16	**26**	95.22 ± 3.30
9	96.62 ± 0.54	**27**	92.97 ± 2.72
10	39.71 ± 3.27	**28**	102.55 ± 3.06
11	96.27 ± 4.14	**29**	98.20 ± 0.37
12	74.89 ± 1.58	**30**	46.84 ± 3.02
13	77.66 ± 6.40	**31**	98.51 ± 0.97
14	95.05 ± 2.78	**32**	83.55 ± 1.51
15	97.90 ± 1.74	**33**	88.55 ± 3.20
16	97.01 ± 1.83	**34**	98.26 ± 1.03
17	98.36 ± 1.65	**35**	90.74 ± 5.24
18	95.05 ± 2.30	[a]**control**	100.00 ± 1.31

[a] control:blank control.

Preprints (www.preprints.org) | NOT PEER-REVIEWED | Posted: 21 November 2023 doi:10.20944/preprints202311.1185.v1

Table 4. Inhibitory effects of compounds **5**, **8**, **10** and **30** on HGC27 cells (mean ± SD, n= 3).

Compound	IC_{50} (%)
5	10.24 ± 0.89
8	28.94 ± 0.72
10	6.08 ± 0.34
30	33.76 ± 2.64

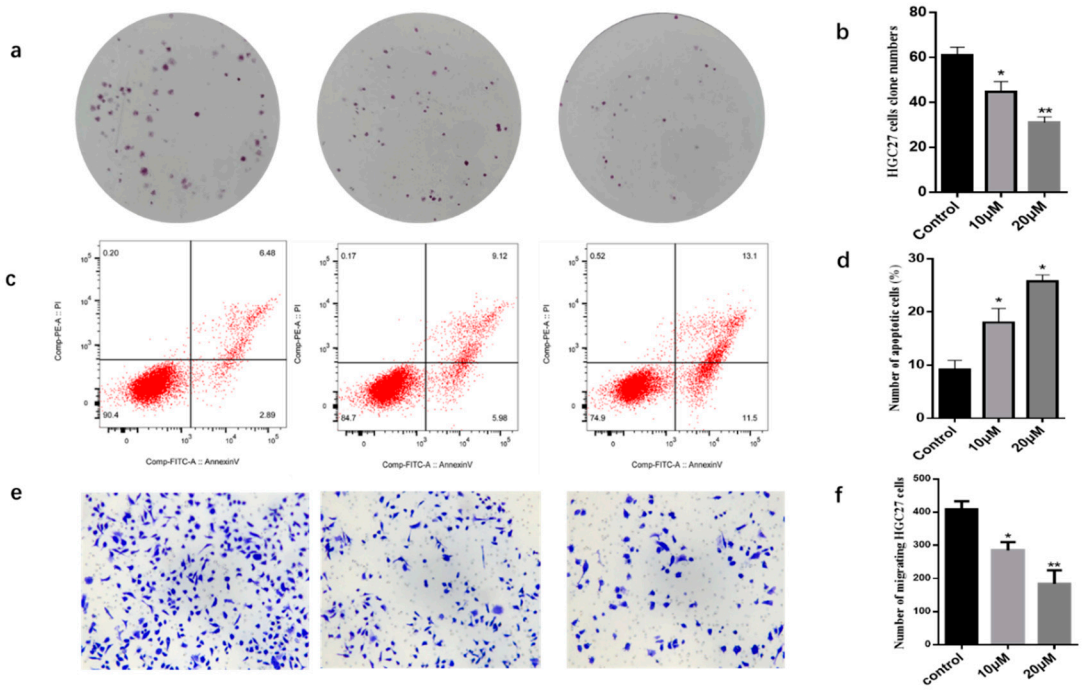

Figure 3. Cells apoptosis and migration assay. **a.** Visual observation of cell clonogenicity. **b**. Statistical analysis of cell clonogenicity. Data are mean±SD (n=3). Differences between treatment groups and control groups are determined,*p< 0.05, **p< 0.01 as compared with control. **c**. Apoptosis caused by **10** in HGC27 cells. **d**. Treatment groups cells apoptosis rate were compared with control, *p< 0.05, Data are expressed as mean ±SD (n=3).**e.** the migration of HGC27 cells, **f**. Quantitative evaluations of cell migration induced by **10** in the transwell assay, treatment groups were compared with control, *p< 0.05, **p< 0.01.Data are expressed as mean ±SD (n=3). Note:control: blank control group, 10μM: 10μmol/mL group, 20μM: 20μmol/mL group.

Cell migration is an essential process in tumor metastasis. The effect of compound **10** on migration was examined by the transwell method. The effect of compound **10** on the migration of HGC27 tumor cells was investigated in the premise of HGC27 cell death. As shown in (Figure 3e), in vitro migration studies showed that compound **10** significantly inhibited the migratory ability of HGC27 cells in a dose-dependent manner. The number of migrating HGC27 cells was reduced from 293 to 66 compared to the control group (Figure 3f). Caspase-3 is an important protein in the regulation of cell apoptosis. Western blot analysis showed after treating HGC27 cells with 10 μM and 20 μM of compound **10** for 48 h, the expression of apoptosis-related protein Caspase-3 was significantly increased compared with the control (Figure 4). Thus compound **10** had a substantial cytotoxic effect on HGC27 cells (Figure 4). We also analyzed Bax and Bcl-2 in the Bcl-2 family protein related to mitochondrial membrane permeability. As an inhibitor of apoptosis, Bcl-2 protein can stabilize mitochondrial membrane potential, while Bax protein can bind to Bcl-2 to form a dimer, thus playing an antagonistic role in Bcl-2 and promoting apoptosis. In addition, the dimer formed by Bax self-binding can also cause changes in cell membrane permeability, thereby reducing mitochondrial membrane potential and eventually leading to apoptosis (Figure 4). After treating HGC27 cells with

Preprints (www.preprints.org) | NOT PEER-REVIEWED | Posted: 21 November 2023 doi:10.20944/preprints202311.1185.v1

10 μM and 20 μM compound **10** for 48 h the expression of Bax in cells increased significantly, while the expression of Bcl-2 in cells decreased (Figure 4). Therefore, compound **10** may induce apoptosis through the mitochondrial apoptosis pathway.

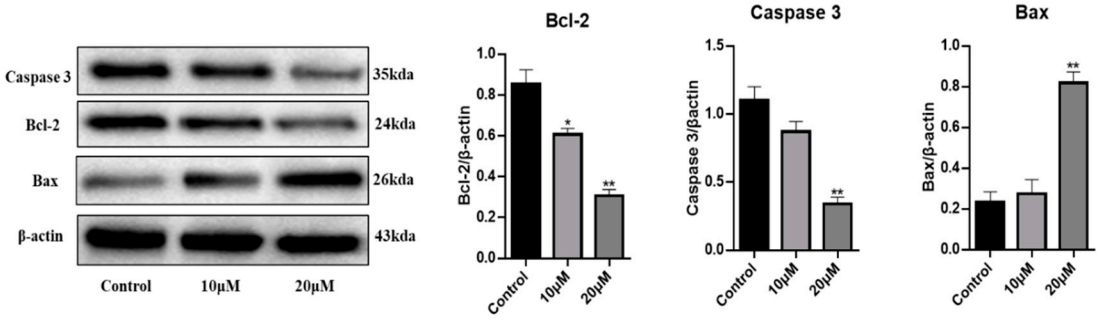

Figure 4. Compound **10** influences the expression of relevant proteins. Detection of Caspase-3 ,Bcl-2 and Bax protein proteins expression level in HGC27cells by Western Blot,the treatment groups were compared with control,*p< 0.05, **p< 0.01.Data were expressed as mean ± SD (n=3). Note:control: blank control group, 10μM: 10μmol/mL group, 20μM: 20μmol/mL group.

3. Experimental

3.1. General experimental procedures

Optical rotations were measured on a Perkin-Elmer 341 polarimeter (Perkin-Elmer Corporation, Wellesley, MA, USA). IR and UV spectra were recorded using a PerkinElmer 1725X-FT spectrometer with KBr disks and a PerkinElmer Lambda 35 spectrometer, respectively. 1D and 2D NMR spectra were recorded on Bruker Avance 400 and 600 spectrometers. High resolution electrospray ionization mass spectrometry (HR-ESI-MS) was performed on a micrOTOF-QII mass spectrometer. TLC was carried out on precoated silica gel GF254 (10 – 40 μm, Qingdao Marine Chemical Group Co., Ltd. Qingdao, China). Analytical HPLC was carried out on Prominence LC-20AT with a model SPD-M20A detector and Ultimate ®C_{18} column (250 mm × 4.60 mm, 5 μm). Preparative HPLC was carried out on P3000 with a UV3000 detector (Chengdu LaiPu Science and Technology Co., Ltd, China) and Ultimate ®C_{18} column (250 mm × 21.2 mm, 5 μm; 250 mm × 50 mm, 10 μm, respectively). Silica gel (100-200, 200-300 mesh, Qingdao Marine Chemical Group Co., Ltd. Qingdao, China). All chemical solvents were obtained from Chron Chemicals Reagent of Chengdu.

3.2. Plant material

The root bark of *M. alba* (Sang-Bai-Pi) was purchased in September 2019 from Lotus Pond Chinese Herbal Medicine market, Sichuan, China, and identified by Professor Weikai Bao (Chengdu Institute of Biology, Chinese Academy of Sciences). A voucher specimen (CIB-A-431) has been deposited at the Laboratory of Phytochemistry, Chengdu Institute of Biology, Chinese Academy of Sciences.

3.3. Extraction and isolation

The dried root bark of *M. alba* (30.0 kg) were crushed into powder, and extracted three times with 75% ethanol (100 L × 3, each 3 days). The resulting solution was filtered, combined and concentrated under reduced pressure to give 3.0 Kg of brown residue. The 75% ethanol extract (3.0Kg) was partitioned between H_2O and ethyl acetate. Tthyl acetate part (2.2 Kg) was obtainedand separated by silica gel column (6.0 Kg, 150 × 40 cm) eluted with petroleum and ethyl acetate (10: 1 to 1: 1) to yield four fractions (Fr.1-4).

Part of Fr.1 (88.0 g) was subjected to preparative reversed-phase HPLC (MeOH - H_2O, 88:12) to afford seven subfractions (Fr.1.1-Fr.1.7). Compound **13** (6.0 g) was obtained from Fr.1.2 (8.3 g) by crystallization. Fr.1.3 (2.0 g) was fractionated with preparative reversed-phase HPLC (MeOH-H_2O,

 doi:10.20944/preprints202311.1185.v1

72:28) to give compounds **1** (22.0 mg)**, 26** (120.0 mg), **11** (8.0 mg)**, 12** (6.6 mg) and **16** (16.0 mg). Compound **15** (8.0 g) was isolated from Fr.1.4 (12.2 g) by crystallization. Compound **2** (310.0 mg**)** was obtained from Fr.1.5 (1.6 g) by preparative reversed-phase HPLC (CH_3CN-H_2O, 64:36). **14** (22.4 g) was isolated from Fr.1.6 (28.9 g) by crystallization. Compounds **17** (18.0 mg), **3** (130.0 mg), **18** (30.0 mg), **19** (46.0 mg), **4** (22.0 mg), **20** (36.0 mg) were separated from Fr.1.7 (503.0 mg) by preparative reversed-phase HPLC (CH_3CN-H_2O, 70:30).

Part of Fr.2 (33.0 g) was subjected to preparative reversed-phase HPLC (MeOH-H_2O, 86:14) to yield six subfractions (Fr.2.1-Fr.2.6). Fr.2.2 (3.8 g) was further purified by preparative reversed-phase HPLC (CH_3CN-H_2O, 70:30) to get **28** (109.0 mg). **21** (28.0 mg) was isolated from Fr.2.4 (1.3 g) by preparative reversed-phase HPLC (MeOH-H_2O, 89:11). Fr.2.5 (300.0 mg) and Fr.2.6 (653.0 mg) was further purified by preparative reversed-phase HPLC (MeOH-H_2O, 90:10) and (MeOH-H_2O, 84:16) to yield **27** (17.0 mg) and **22** (100.0 mg), respectively.

Part of Fr.3 (12.6 g) was subjected to preparative reversed-phase HPLC (MeOH-H_2O, 86:14) to get six subfractions (Fr.3.1- Fr.3.7). Compounds **31** (15.7 mg), **30** (8.0 mg), and **7** (33.0 mg) were separated from Fr.3.1 (817.0 mg) through preparative reversed-phase HPLC (MeOH-H_2O, 73:17). **23** (86.0 mg) and **5** (42.0 mg) were purified from Fr.3.2 (310.0 mg) by preparative reversed-phase HPLC (CH_3CN-H_2O, 63:27). **24** (28.0 mg) was obtained from Fr.3.3 (120.0 mg) by preparative reversed-phase HPLC (CH_3CN-H_2O, 60:40). Fr.3.4 (800.0 mg) was further purified by preparative reversed-phase HPLC (CH_3CN-H_2O, 64:36) to afford **6** (98.0 mg). Fr.3.5 (900.0 mg) was purified by preparative reversed-phase HPLC (MeOH-H_2O, 78:22) to give **29** (37.0 mg).

Part of Fr.4 (36.0 g) was subjected to preparative reversed-phase HPLC (CH_3CN-H_2O, 64:36) to yield six subfractions (Fr.4.1-Fr.4.6). Fr.4.2 (13.6 g) was separated by preparative reversed-phase HPLC (CH_3CN-H_2O, 63:37) to afford **33** (303.0 mg), **34** (23.0 mg), and **35** (6.0 mg). Fr. 4.3 (800.0 mg) was purified by preparative reversed-phase HPLC (CH_3CN-H_2O, 45:55) to give **9** (168.0 mg). Compound **8** (40.0 mg) was further purified from Fr.4.5 (500.0 mg) by preparative reversed-phase HPLC (CH_3CN-H_2O, 52:48). Fr.4.6 (200.0 mg) was separated by preparative reversed-phase HPLC (CH_3CN-H_2O, 62:38) to yield **32** (160.3 mg). Compounds **10** (128.0 mg) and **25** (36.0 mg) were separated from Fr.4.7 (1.6 g) through preparative reversed-phase (MeOH-H_2O, 74:26).

3.4. Spectroscopic data

Compound **1**, Brown amorphous powder, $[\alpha]_D^{20}$ + 3.0 (c 0.22, MeOH); UV (MeOH) λ_{max} (log ε) 216 (4.21), 316 (4.19) nm; IR (KBr) ν_{max} 3423, 1615, 1490, 1362, 1266, 1155, 1084 cm^{-1}; HR-ESI-MS at *m/z* 431.1831 $[M + Na]^+$ (calcd. for $C_{25}H_{28}O_5Na$, 431.1829); ^1H and ^{13}C NMR data, see Table 1.

Compound **11,** Yellow powder, $[\alpha]_D^{20}$ + 3.7 (c 0.22, MeOH); UV (MeOH) λmax (log ε) 216 (3.21), 327 (4.36) nm; IR (KBr) ν_{max} 3415, 1656, 1621, 1554, 1448 cm^{-1}; HRESIMS *m/z* 439.1751 $[M + H]^+$ (calcd. for $C_{25}H_{27}O_7$, 439.1751); ^1H and ^{13}C NMR data, see Table 2.

Compound **12,** Yellow amorphous powder, $[\alpha]_D^{20}$ + 10.6 (c 0.22, MeOH); UV (MeOH), λmax (log ε) 215 (2.61), 336 (3.18) nm; IR (KBr) ν_{max} 3372, 1645, 1616, 1440, 1299, 1167 cm^{-1} ; HRESIMS *m/z* 439.1751 $[M + H]^+$ (calcd. for $C_{25}H_{27}O_7$, 439.1749); ^1H and ^{13}C NMR data, see Table 2.

3.5. Cell culture

HGC27 cells were bought from American Type Culture Collection (ATCC). All cells grew adherently. HGC27 cells were cultured in RPMI 1640 media, and MRC-5 cells were cultured in a minimal essential medium (Gibco). All media contained 10% endotoxin-free, heat-inactivated FBS (Gibco) and were maintained at 37°C in a humidified atmosphere of 5% CO_2. Cell passage was performed in 1:3 when the confluence reached 70%.

3.6. Cytotoxicity assay and CCK-8 assay

HGC27 cell lines (4 × 10^3/well) were seeded in 96-well plates with 200 μL per well and incubated at 37 °C overnight. **35** compounds with more than 96% purity were prepared in our own laboratory. **35** compounds were first dissolved in DMSO (Sigma). Then they were diluted with the corresponding

medium into 1 mg/mL concentration and stored at -20 °C. The final concentration of DMSO for all treatments was less than 0.1%. Cells were treated with the isolated compound (**1**-**35**) 10μM for 24h. Then, 10μL of CCK-8 reagent (biofrox Z6789D144) was added into each well, and incubated for 4 h at 37 °C. Finally, the optical density (OD) was then measured at 450 nm. Cell viability was calculated as follows: cell viability = (OD experiment – OD blank) / (OD control – OD blank) × 100%.

Cells were treated with varying concentrations of compounds **5**, **8**, **10** and **30** (1, 2.5, 5, 10, 20, 30 40 and 60μM) for 24h. Then, 10μL of CCK-8 reagent (biofrox Z6789D144) was added into cells, and incubated for 4 h at 37 °C. Finally, the absorbance was measured at 490 nm, and the IC_{50} values were calculated.

3.7. Colony Formation Assay

Colony formation assay was performed as described previously. Briefly, 500 cells per well were seeded in 12-well plates and allowed to adhere to the plate for 24 h, and then ABN-B was added to the wells at different concentrations. Following 48 h incubation, the medium was replaced with fresh medium with or without ABN-B, and the cells were further grown for an additional five days. After the cells were washed with PBS (pH 7.4) twice, the cells were stained with crystal violet solution (0.1%) diluted in ethanol 40% for 5 min. Then, the stain solution was removed using tap water, and the cells were air-dried. Finally, the number of colonies was counted.

3.8. Cell apoptosis assay

HGC27 cells were cultured in a 6-well plate at a density of 700,000 cells / well and incubated in a cell incubator for 24 h. When HGC27 cells were in the logarithmic growth phase, HGC27 cells were treated with 10 μM or 20 μM compound **10** for 48 h. Then cells were collected by trypsin digestion without EDTA and washed twice with cold PBS. 5 μL Annexin V / Alexa Fluor 488 solution was added to the cell suspension and incubated in the dark at room temperature for 5 min. Then 10 μL PI and 400 μL PBS solution were added. The stained cell suspension was transferred to a flow tube, and the proportion of apoptotic cells was detected using BD Facscanto II (BD Biosciences, USA), and the experimental results were statistically analyzed using Flowjo.

3.9. Transwell migration assay

Before the experiment, the cells were starved by culturing in a serum-free medium for 4 hours. Then, cells were collected, and 30, 000 cells were cells were treated with 10μM and 20μM Compound **10** inoculated into 500 μL serum-free medium in the upper chamber of Transwell (Corning), and 500μl culture medium with 10% FBS was added into the lower chamber. After 24 hours of incubation, the culture medium was discarded. Fixed with 4% paraformaldehyde (Beyotime, China) for 15 minutes, then stain with 0.4% crystal violet (Beyotime, China) for 15 minutes. The cells were observed and photographed under a light microscope.

4.10. Western Blot Analysis

Briefly, HGC27 cells in logarithmic growth phase were digested with trypsin, and after resuspended, adjusted to a density of 4×10^5/mL, and inoculated into six-well plate with 2 mL in each well. When the cells grew to about 50%, the original medium was aspirated, and the medium containing 0.1% DMSO, 10 μM, and 20 μM compound **10** was added, respectively. A total of 4 groups: blank control group, 0.1%DMSO group, 10 μM group, and 20 μM group. Cell protein was extracted after 24 h. Protein concentration was measured using a BCA protein assay kit (Biosharp, Guanzhou, China). Next, equal amounts of proteins were separated by sodium dodecyl sulfate-polyacrylamide gel electrophoresis (SDS-PAGE) and then transferred to polyvinylidene fluoride (PVDF) membranes (Millipore, USA). After blocked with 5% non-fat milk for 1 h at room temperature (RT), the membranes were incubated with the specific primary antibodies (Signalway Antibody, Nanjing, China) overnight at 4°C. After washing 3 times with Tris Buffered saline Tween 20 (TBST), the membranes were then incubated with horseradish peroxidase (HRP)-conjugated secondary

antibodies (ProteinTech, Wuhan, China) for 1h at RT. The immune-blotting signals were detected using Beyo ECL Plus electrochemiluminescence reagent (Beyotime, Shanghai, China).

4. Conclusions

Phytochemical investigation of the 75% ethanol extract of the root bark of *M. alba* led to the isolation and identification of three new compounds (**1**, **11** and **12**) and 32 known ones (**2–10**, **13–35**). All compounds were tested for their cytotoxic activities against gastric cancer HGC27 cells. As a result, compounds **5**, **8** and **30** exhibited certain degree cytotoxic activities with the IC_{50} values ranging from 10.24±0.89 μM, 28.94±0.72 μM and 33.76 ±2.64 μM, respectively. Compound **10** showed the significant cytotoxic activity with an IC_{50} value of 6.08 ± 0.34 μM. Then compound **10** was subjected to further experiments to explore its anti-tumor mechanism. It was found that compound 10 has inhibitory effects on proliferation and migration of human cancer HGC27 cells. In addition, compound **10** induced up-regulation of Bax protein expression and down-regulation of Caspase-3 and Bcl-2 protein expression, which may be related to mitochondrial dysfunction and decreased mitochondrial membrane potential. Therefore, we hypothesized that compound **10** could induce apoptosis of HGC27 cells through the mitochondrial apoptotic pathway. Here, This study was the first time to preliminarily explore the mechanism of compound 10 in inhibiting gastric cancer cell HGC27 in vitro. In conclusion, the present study provides a reference for the phytochemical and biological activities of *Morus alba L*.

References

1. State Pharmacopoeia Committee. Chinese Pharmacopoeia; China Medical Pharmaceutical Science and Technology Publishing House: Beijing, China. 2010, p182.
2. Asano, N.; Yamashita, T; Yasuda, K.; Ikeda, K.; Kizu, H.; Kameda, Y.; Kato, Nash, A. R.J.; Lee, H.S.; Ryu, K.S. Polyhydroxylated alkaloids isolated from mulberry trees (*Morus alba L.*) and silkworms (*Bombyx mori L.*). J. Agric. Food. Chem. 2001, 49, 4208-4213.
3. Čulenová, M.; Sychrová, A.; Hassan, S.T.S.; Berchová-Bímová, K.; P. Svobodová, P.; Helclová, A.; Michnová, H.; Hošek, J. Multiple In vitro biological effects of phenolic compounds from *Morus alba* root bark. J. Ethnopharmacol. 2020, 248, 112296.
4. Zhang, Q.J.; Li, D.Z.; Chen, R.Y.; Yu, D.Q. A new benzo-furanolignan and a new flavonol derivative from the stem of *Morus australis*. Chin. Chem. Lett. 2008, 19, 196–198.
5. Takahashi, M.; Takara, K.; Toyozato, T.; Wada, K. A novel bioactive chalcone of *Morus australis* inhibits tyrosinase activity and melanin biosynthesis in B16 melanoma cells. J. Oleo Sci. 2012, 61, 585–592.
6. Ko, H.H.; Wang, J.J.; Lin, H.C.; Wang, J.P., Lin, C.N. Chemistry and biological activities of constituents from *Morus australis*. Biochim. Biophys. Acta. Gen. Subj. 1999, 1428, 293-299.
7. Zheng, Z.F.; Zhang, Q.J.; Chen, R.Y.; Yu, D.Q. Four new flavonoids from *Morus australis*. J. Asian. Nat. Prod. Res. 2012, 14 3, 263-269.
8. Zhang, Q.J.; Tang, Y.B.; Chen, R.Y.; Yu, D.Q. Three new cytotoxic Diels-Alder-type adducts from *Morus australis*, Chem. Biodivers. 2007, 4, 1533-1540.
9. Zhang, Q.J.; Zheng, Z.F.; Chen, R.Y.; Yu, D.Q. Two new dimeric stilbenes from the stem bark of *Morus australis*. J. Asian. Nat. Prod. Res, 2009, 11, 138-141.
10. Kikuchi, T.; Nihei, M.; Nagai, H.; Fukushi, H.; Tabata, K.; Suzuki, T.; Akihisa, T. Albanol A from the root bark of *Morus alba L.* induces apoptotic cell death in HL60 human leukemia cell line. Chem. Pharm. Bull. 2010, 58, 568–572.
11. Cui, L.; Lee, H S.; Oh, W K.; Ahn J S. Inhibition of sangginon G isolated from *Morus alba* on the metastasis of cancer cells. Chin. Herb. Med. (2011), 3, 23–26.
12. Agabeyli, R A.; Antimutagenic activities extracts from leaves of the *Morus alba*, *Morus nigra* and their mixtures. Intl. J. Biol. 2012, 4, 166–172.
13. Devi, B.; Sharma, N.; Kumar, D.; Jeet, K. *Morus alba L* inn: a phytopharmacological review. Int. J. Pharm. Pharma. Sci. 2013, 5, 14–18.
14. Hong, S S.; Hong, S.; Lee, H J.; Mar, W.; Lee, D A. A new prenylated flavanone from the root bark of *Morus*. B. Korean. Chem. Soc. 2013, 34, 2528–2530.

15. Zhang, X.R.; Wang, S.Y.; Sun, W.; Wei C. Isoliquiritigenin inhibits proliferation and metastasis of MKN28 gastric cancer cells by suppressing the PI3K/AKT/mTOR signaling pathway. Mol. Med. Rep. 2018, 18, 3429-3436.
16. Li, Y.W.; Xu, Y.Q.; Lei, B.; Wang, W.X.; Ge, X.; Li, J.R. Rhein induces apoptosis of human gastric cancer SGC-7901 cells via an intrinsic mitochondrial pathway. Braz. J. Med. Biol. Res. 2012, 45, 1052-1059.
17. Nomura, T.; Fukai, T.; Shimada, T.; Chen, I.S. Mulberrofuran D, a new isoprenoid 2-arylbenzofuran from the root barks of the mulberry tree *(Morus australis Poir*.). Heterocycies. 1982, 19, 1855-1860.
18. Chang, Y.S.; Jin, H.G.; Lee, H.; Lee, D.S.; Woo, E.R. Phytochemical constituents of the root bark from *Morus alba* and their Il-6 Inhibitory activity. Nat. Prod. Sci. 2019, 25, 268-274.
19. Wu, D.L.; Zhang, X.Q.; Huang, X.J.; He, X.M.; Wang, G.C.; Ye, W.C. Chenucal constituents from root barks of *Morus atropurpurea*. J. Chin. Med. Mater. 2010, 35, 1978-1982.
20. Jeong, S.H.; Ryu, Y. B.; Curtis-Long, M. J.; Ryu, H. W.; Baek, Y. S.; Kang, J. E.; Lee, W.S.; Park, K.H. Tyrosinase Inhibitory polyphenols from roots of *Morus Ihou*. J. Agric. Food. Chem. 2009, 57, 1195-1203.
21. Shi, Y. Q.; Fukai, T.; Sakagami, H.; Chang, W.J.; Yang, F.Q.; Wang, F.P.; Nomura, T. Cytotoxic flavonoids with isoprenoid groups from *Morus mongolica*. J. Nat. Prod. 2001, 64, 181-188.
22. X. He, X. Chao, L. Yang, C. Zhang, R. Pi, H. Zeng, G. Li, Y. Xu, Y. Lin, The research on chemical ingredients of the heartwood of root of *Morus atpropurpurea*, Nat. Prod. Res. Dev. 2014 26 (2) (2014) 193-196.
23. Jung, J.W.; Koo, W.M.; Park, J.H.; Seo, K.H.; Oh, E.J.; Lee, D.Y.; Lee, D.S.; Kim, Y.C.; Lim, D.W.; Han, D.; Baek, N.I. Isoprenylated flavonoids from the root bark of *Morus alba* and their hepatoprotective and neuroprotective activities. Arch. Pharm. Res. 2015, 38, 2066–2075.
24. Cui, X.Q.; Chen, H.;. Chen, R.Y. Study on Diels-Alder type adducts from stem bark of *Morus yunanensis*. J. Chin. Med. Mater. 2009, 34, 286-290.
25. Cui, X.Q.; Wang, H.Q.; Liu, C.; Chen, R.Y. Study on anti-oxidant phenolic compounds from stem bark of *Morus yunanensis*. J. Chin. Med. Mater. 2008, 13, 1569-1572.
26. He, X.M; Wu, D.L.; Zou, Y.X; Wang, G.C.; Zhang, X.Q.; Liao, S.T.; Sun, J.; Ye, W.C. Chemical constituents from root barks of *Morus atropurpurea*. J. Chin. Med. Mater. 2010, 35, 1978-1982.
27. Zhen, P.; Ni, G.; Guo, W,Q.; Shi, G.R,; Chen, R.Y.; Yu, D.Q. Isolation and identification of pharmaceutical chemical constituents from branches of *Morus notabilis*. Science of Sericulture. 2016, 42, 0307-0312
28. Guo, Y.Q.; Tang, G.H.; Lou, L.L.; Li, W.; Zhang, B.; Liu, B.; Yin, S. Prenylated flavonoids as potent phosphodiesterase-4 inhibitors from *Morus alba*: Isolation, modification, and structure-activity relationship study. Eur. J. Med. Chem. 2018, 144, 758-766.
29. Kim, J.Y.; Lee, W.S., Kim, Y.S., Marcus J., C.L.; Lee, B.W.; Ryu, Y. B.; Park, K.H. Isolation of cholinesterase-Inhibiting flavonoids from *Morus lhou*. J. Agric. Food. Chem. 2011, 59, 4589-4596.
30. Geng, C.A.; Yao, S.Y.; Xue, D.Q.; Zuo, A.; Zhang, X.M; Jiang, Z.Y.; Ma, Y.B.; Chen, J.J. New isoprenylated flavonoid from *Morus alba*. J. Chin. Med. Mater. 2010, 35, 1560-5.
31. Tseng, T.H.; Chuang, S.K.; Hu, C.C.; Chang, C.F.; Huang, Y.C.; Lin, C.W.; Lee, Y.J. The synthesis of morusin as a potent antitumor agent. Tetrahedron. 2010, 66, 1335-1340.
32. Fujimoto, T.; Hano, Y.; Nomura, T.; Uzawa, J. Components of root bark of cudrania tricuspidata 2. Structures of two new isoprenylated flavones, Cudraflavones A and B. Planta. Med. 1984, 50, 161-163.
33. Guo, S.; Liu, L.; Zhang, S.S.; Yang, C.; Yue, W.P.; Zhao, H.A.; Ho, C.T.; Du, J.F.; Zhang, H.; Bai, N.S. Chemical characterization of the main bioactive polyphenols from the roots of *Morus australis* (mulberry). Food. Funct. 2019, 10, 6915-6926.
34. Wang, L.; Yang, Y.; Liu, C.; Chen, R.Y. Three new compounds from *Morus nigra L*. J. Asian. Nat. Prod. Res. 2010, 12, 431-437.
35. Zheng, Z.P.; Tan, H.Y.; Wang, M.F. Tyrosinase inhibition constituents from the roots of *Morus australis*. Fitoterapia. 2012, 83, 1008-1013.
36. Qin, J.; Fan, M.; He, J.; Wu, X.D.; Peng, L.Y. , Su, J.; Cheng, X.; Li, Y.;. Kong, L.M; Li, R.T.; Zhao, Q.S. New cytotoxic and anti-inflammatory compounds isolated from *Morus alba L*. Nat. Prod. Res. 2015, 29, 1711-1718.
37. Patil, A.D.; Freyer, A.J.; Killmer, L.; Offen, P.; Taylor, P.B.; Votta, B.J.; Johnson, R.K. A new dimeric dihydrochalcone and a new prenylated flavone from the bud covers of *Artocarpus altilis*: potent inhibitors of cathepsin K. J. Nat. Prod. 2002, 65, 624-627.
38. Yang, D.S.; Li, Z.L.; Yang, Y.P.; Xiao, W.L.; Li, X.L. New geranylated 2-Arylbenzofuran from *Morus alba*. Chin. Herb. Med. 2015, 7, 191-194.

39. Zuo, G.Y.; Yang, C.X.; Ruan, Z.J.; Han, J.; Wang, G.C. Potent anti-MRSA activity and synergism with aminoglycosides by flavonoid derivatives from the root barks of *Morus alba*, a traditional chinese medicine. Med. Chem. Res. 2019, 28, 1547-1556.
40. Nomura, T.; Fukai, T.; Sato, E.; Fukushima, K. The formation of moracenin-D from kuwanon-G. Heterocycles. 1981, 16, 983-986.
41. Hano, Y.; Yamanaka, J.; Momose, Y.; Nomura, T. Sorocenols C-F, four new isoprenylated phenols from the root bark of *Sorocea bonplandii Baillon*. Heterocycles. 1995, 41, 2811-2821.
42. Liu, Y.J.; Wu, J.C.; Li, H.L.; Ma, Q.; Chen, Y.G. Alkaloid and flavonoids from the seeds of *Whitfordiodendron filipes*. Chem. Nat. Compd. 2016, 52, 188-190.
43. Shi, Y. Q.; Fukai, T.; Sakagami H. Cytotoxic flavonoids with isoprenoid groups from *Morus m ongolica*. J. Nat. Prod. 2001, 64, 181-188.
44. Zhang, Y.L.; Luo, J.G.; Wan, C.X.; Zhou, Z.B.; Kong, L.Y. Geranylated 2-arylbenzofurans from *Morus alba* var. tatarica and their α-glucosidase and protein tyrosine phosphatase 1B inhibitory activities. Fitoterapia. 2014, 92, 116–126.
45. Jin, Y.J.; Lin, C.C.; Lu, T.M.; Li, J.H.; Chen, I.S.; Kuo, Y.H.; Ko, H.H. Chemical constituents derived from *Artocarpus xanthocarpus* as inhibitors of melanin biosynthesis. Phytochemistry. 2015, 117, 424–435.
46. Tuan Hiep, N.Y.; Kwon, J.Y.; Hong, S.G.; Kim, N.Y.; Guo, Y.Q.; Hwang, B.Y.; Mar, W.C.; Lee, D.H. Enantiomeric isoflavones with neuroprotective activities from the fruits of *Maclura tricuspidata*. Sci.Rep. 2019, 9, 1757.